iScience

Article

# Are there changes in the foot biomechanics during the before and after fifth metatarsal fracture running stance phase?

## Graphical abstract

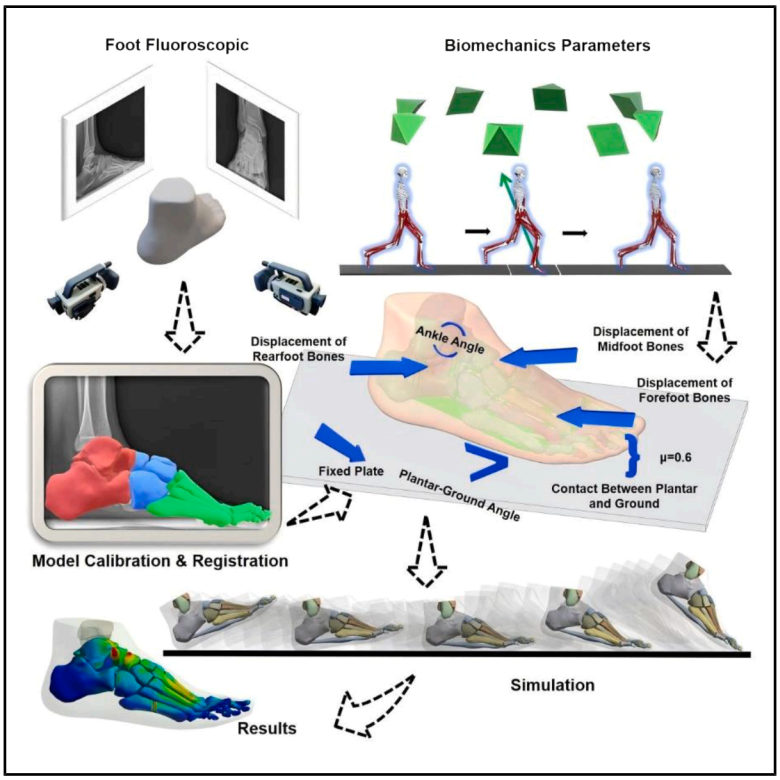


## Authors

Huiyu Zhou, Datao Xu, Wenjing Quan, Zixiang Gao, Liangliang Xiang, Yaodong Gu

## Correspondence

guyaodong@nbu.edu.cn

## In brief

Health sciences; Sports medicine; Health technology; Biomechanics

## Highlights

- Restoring pre-MT5 fracture foot kinematic state
- Compensatory foot motion mechanisms post-MT5 fracture
- Foot bone displacement changes following MT5 fracture
- Rehabilitation outcome evaluation post-MT5 fracture

Zhou et al., 2025, iScience *28*, 112432
May 16, 2025 
https://doi.org/10.1016/j.isci.2025.112432

CellPress

iScience

CellPress
OPEN ACCESS

Article

# Are there changes in the foot biomechanics during the before and after fifth metatarsal fracture running stance phase?

Huiyu Zhou,[1] Datao Xu,[1] Wenjing Quan,[1] Zixiang Gao,[2] Liangliang Xiang,[3] and Yaodong Gu[1,4,*]
[1]Faculty of Sports Science, Ningbo University, Ningbo 315211, China
[2]Human Performance Laboratory, Faculty of Kinesiology, University of Calgary, Calgary, AB, Canada
[3]KTH MoveAbility Lab, Department of Engineering Mechanics, KTH Royal Institute of Technology, Stockholm, Sweden
[4]Lead contact
*Correspondence: guyaodong@nbu.edu.cn
https://doi.org/10.1016/j.isci.2025.112432

## SUMMARY

The purpose of this study is to restore the before fracture kinematic state by using the observed foot bone displacements as boundary conditions for finite element (FE) analysis. Secondly, this study aims to compare the biomechanical changes of the foot before and after a metatarsal (MT) fracture using this method. A total of 21 subjects had previously experienced a shaft stress fracture of the MT5 in the six months before the collection of experimental data. All patients received treatment through the use of cast immobilization for duration of 4–6 weeks. After the subject's recovery, we obtained gait biomechanical data. At the same time, we also obtained gait data from 21 healthy subjects as the control group. This study found that when a fracture of the MT5 occurs, even after rehabilitation, there is a significant impact on the metatarsal.

## INTRODUCTION

Running has gained significant popularity due to its straightforward nature and easy accessibility, resulting in a steady rise in the number of individuals engaging in this form of physical exercise each year.[1] However, this also raises the issue of an increasingly high incidence of running-related injuries.[2–4] Foot-related injuries constitute a significant proportion of all injuries to the lower extremities, including fractures of the metatarsal (MT) bones. Fractures of the fifth MT are the prevailing MT fractures in individuals over the age of 5, including both children and adults. Between 45% and 70% of MT fractures concentrate on the MT5.[5–8] We can categorize the fractures into three types: tuberosity avulsion fractures, Jones fractures at the metaphyseal-diaphyseal junction, and shaft stress fractures.[9,10] Shaft stress fractures are pathological fractures primarily observed in athletes but can also occur in individuals with weak bone structure.[11]

The human foot is a highly resilient mechanical structure, consisting of 26 bones, 33 joints, and a variety of muscles, tendons, ligaments, cartilage, and other tissues. The foot acts as the initial connection between the internal kinetic chain of the human body and the external movement environment. This occurs not only during static standing but also during dynamic activities such as walking and running et al..[12–16] Being the only part of the human kinetic chain that comes into contact with the ground, any modification in the structure of the foot directly influences the modified movement patterns of the foot and lower limbs. Therefore, when a fracture occurs in this crucial structure, it will adversely affect the functioning of the entire lower limb, much like a problem with the root of a tree that inevitably leads to issues with the trunk of the same tree. Competitive athletes may need surgical intervention if the MT5 fracture displaces more than 3 mm or angulates more than 10° in either dorsiflexion or plantarflexion. Alternatively, if surgery is not chosen, non-surgical treatment entails immobilizing the affected area without applying any pressure to it for duration of up to 3 months.[11]

With the significant improvement in computer technology and programming capabilities in recent years, academic and industrial fields have made significant progress in modeling and analyzing complex systems, such as skeletal or mechanical structures, thanks to the use of analog simulation software.[17,18] As a result, finite element (FE) analysis of mathematical models demonstrates greater advantages in terms of cost control, time efficiency, ease of operation, and flexibility compared to traditional experimental methods.[19] FE modeling is gradually finding more and more applications in the biomechanical study of the lower extremity, including the foot and ankle, especially in its ability to assess and predict the risk of gait injuries that may occur during walking, running, and athletic training.[20–23] Recently, several researchers have conducted more in-depth investigations into foot changes using FE and the high-speed dual fluoroscopic imaging system (DFIS) techniques.[24] These techniques allow non-invasive observation of changes in the skeletal structure during exercise, providing a genuine means of directly observing alterations in skeletal kinematics.

Most of the current FE foot research is based on biomechanical testing and boundary conditions calculated by simulation

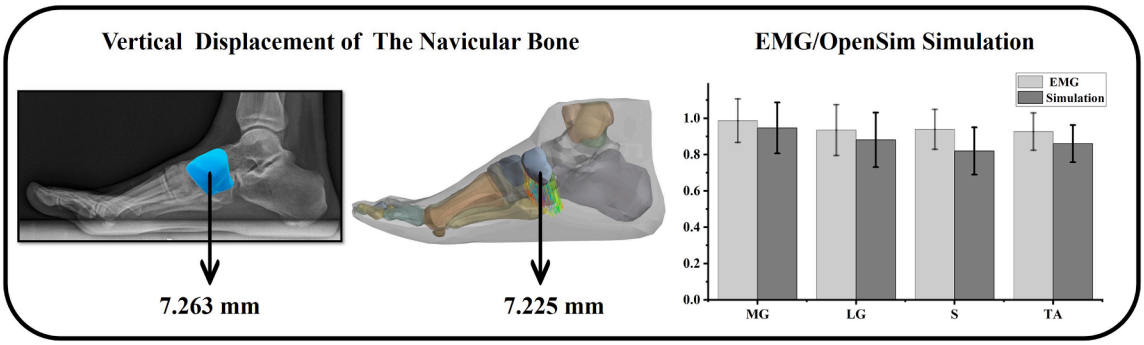


**Figure 1. Validation of the simulation model**
Vertical displacement validation of model; validation of the EMG and OpenSim simulation.

software, but there are significant limitations to this approach. For example, the placement of reflective markers can cause kinematic calculations to be off, impurities on the surface force plate can cause kinetic acquisition to be off, and electrical signal conduction on the skin surface can cause muscle force calculations to be off. Therefore, the purpose of this study is to restore the before fracture kinematic state by using the observed foot bone displacements (DFIS) as boundary conditions for FE analysis. Secondly, the second purpose of this study is to compare the biomechanical changes of the foot before and after MT fracture by this method. Finally, we proceeded to make additional speculations regarding potential biomechanical alterations based on kinematics, kinetics, and muscle forces parameters. We hypothesized that the stresses in MT1-4 would be different before and after the MT5 fracture, and we further hypothesized that perhaps the MT1 stresses would be higher after the fracture than before.

## RESULTS

### Validation of the simulation model

An analysis was conducted to simulate the structure of the foot during running. The obtained results were then compared to the deformation of the navicular bone in order to validate the accuracy of the FE foot model. Since finite element simulation is an engineering method for computers to restore the real situation, in order to determine the accuracy of its results, we verified it through the deformation of the navicular bone. Using 14 datasets, the intraclass correlation coefficient (ICC) were used to assess the level of agreement between *in vivo* measurements and predictions. According to Koo,[25] the ICC estimate was classified as weak below 0.50, moderate between 0.50 and 0.75, strong between 0.75 and 0.9, and excellent reliability beyond 0.90. Our results show that the ICC test displayed an excellent ICC score (0.97). The displacement of the navicular bone is used as an alternative measure for the foot deformation index in clinical settings. The tuberosity of the medial side navicular bone is frequently employed as the point of reference when conducting manual measurements. Figure 1 depicts the comparison between the measured deformation of the navicular bone[26,27] and the result obtained through FE simulation. Figure 1 also shows that the Electromyography (EMG) data and musculoskeletal models compare in terms of muscle activation. Additionally, the optimal quantity of elements and the corresponding nodes were as follows: 146,030 elements and 31,651 nodes before to the MT5 fracture; 151,975 elements and 37,714 nodes after to the MT5 fracture.

### The spatial displacements 21 healthy subjects

Figure 2 illustrates the spatial displacements of three parts of foot segments in a group of 21 healthy subjects during the running stance phase.

### The spatial displacements 21 after fracture subjects

Figure 3 illustrates the spatial displacements of three parts of foot segments in a group of 21 after fracture subjects during the running stance phase.

### The distribution of the Von-Mise stress

Figure 4 illustrates the distribution of the Von-Mise stress changes in the MT1-4 at different running stance phase, from 10% to 90%, respectively. The maximum value of stress in the stance phase is 30.775 MPa while the minimum value is 0.2517 MPa. From 10% to 40% of the stance phase, the stress on the MT gradually shifts from being maximum at the proximal end to being maximum at the middle (50% of the stance phase); from 60% to 90% of the stance phase, the maximum stress transitions from the middle to the distal end, until finally the foot leaves the ground.

### Changes of biomechanical parameters

Figure 5A demonstrates significant differences of the ankle angle (plantarflexion and dorsiflexion: 63.03%–100%, $p < 0.001$; eversion and inversion: 38.47%–79.44%, $p = 0.002$), ankle moment (plantarflexion and dorsiflexion: 22.38%–61.23%, $p < 0.001$) and ankle power (plantarflexion and dorsiflexion: 18.50%–36.56%, $p < 0.001$; 46.57%–75.83%, $p < 0.001$; eversion and inversion: 0.52%–18.17%, $p < 0.001$; 31.07%–56.20%, $p < 0.001$) during the running stance phase for before and after fracture. Figure 5B demonstrates significant differences of the knee angle (eversion and inversion: 58.76%–100%, $p = 0.004$), knee moment (eversion and inversion: 20.75%–25.55%, $p = 0.046$), and knee power (eversion and inversion: 18.16%–29.43%, $p < 0.001$) during the running stance phase for before and after fracture. Figure 5D

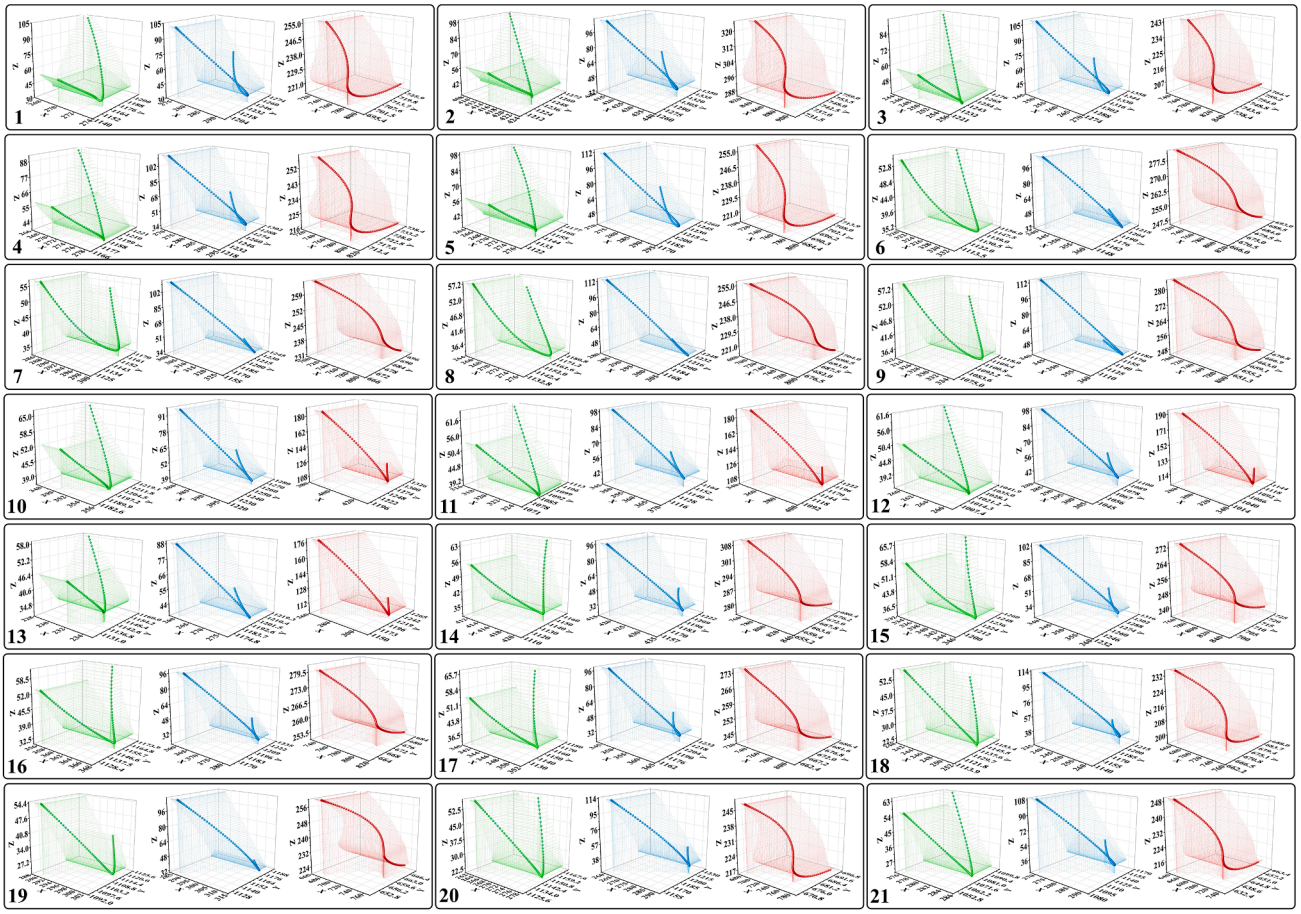

**Figure 2. The spatial displacements 21 healthy subjects**

The spatial displacements of three parts of foot segments in a group of 21 healthy subjects during the running stance phase. Green: forefoot; blue: midfoot; red: rearfoot.

demonstrates significant differences of the ankle joint force (anterior and posterior: 10.10%–14.28%, $p = 0.037$; 24.35%–38.21%, $p = 0.002$; 46.19%–92.56%, $p < 0.001$) (medial andlateral: 30.98%–90.50%, $p < 0.001$) (vertical: 2.73%–29.70%, $p < 0.001$; 37.94%–96.43%, $p < 0.001$) and knee joint force (anterior and posterior: 0.60%–6.69%, $p = 0.020$; 16.21%-21.20, $p = 0.027$; 33.32%–94.75%, $p < 0.001$) (medial and lateral: 30.96%–100%, $p < 0.001$) (vertical: 4.90%–29.42%, $p < 0.001$; 41.87%–95.58%, $p < 0.001$) during the running stance phase for before and after fracture. Figure 5C demonstrates significant differences of soleus (0%–42.76%, $p < 0.001$), tibialis anterior (0%–23.59%, $p < 0.001$; 33.15%–82.16%, $p < 0.001$), medial gastrocnemius (0%–100%, $p < 0.001$), lateral gastrocnemius (0%–27.27%, $p < 0.001$; 30.14%–64.65%, $p < 0.001$; 70.78%–100%, $p < 0.001$), flexor hallucis longus (0%–34.90%, $p < 0.001$; 45.93%–72.55%, $p < 0.001$; 83.20%–100%, $p = 0.006$), extensor hallucis longus (0%–8.53%, $p = 0.030$; 22.46%–33.41%, $p = 0.021$; 38.78%–100%, $p < 0.001$), flexor digitorum longus (0%–38.86%, $p < 0.001$; 48.13%–77.43%, $p = 0.001$; 86.59%–100%, $p = 0.020$), and extensor digitorum longus (16.45%–31.71%, $p = 0.002$) during the running stance phase for before and after fracture. Figure 5E shows the Von-Mises stress change of the MT1-4 during the running stance phase for before and after fracture.

## DISCUSSION

The primary purpose of this study is to restore the before fracture kinematic state by using the observed foot bone displacements (DFIS) as boundary conditions for FE analysis. Secondly, the second purpose of this study is to compare the biomechanical changes of the foot before and after MT fracture using this method. Finally, we proceeded to make additional speculations regarding potential biomechanical alterations based on kinematics, kinetics, and muscle forces parameters. We hypothesized that the stresses in MT1-4 would be different before and after the MT5 fracture, and we further hypothesized that perhaps the MT1 stresses would be higher after the fracture than before. Our hypotheses are in general in agreement with our results, as can be seen in Figures 4 and 5E where the stress of MT1-4 before and after fracture is very different. Secondly, according to the results of Figure 5E, the MT1 stress after fracture is higher than before fracture.

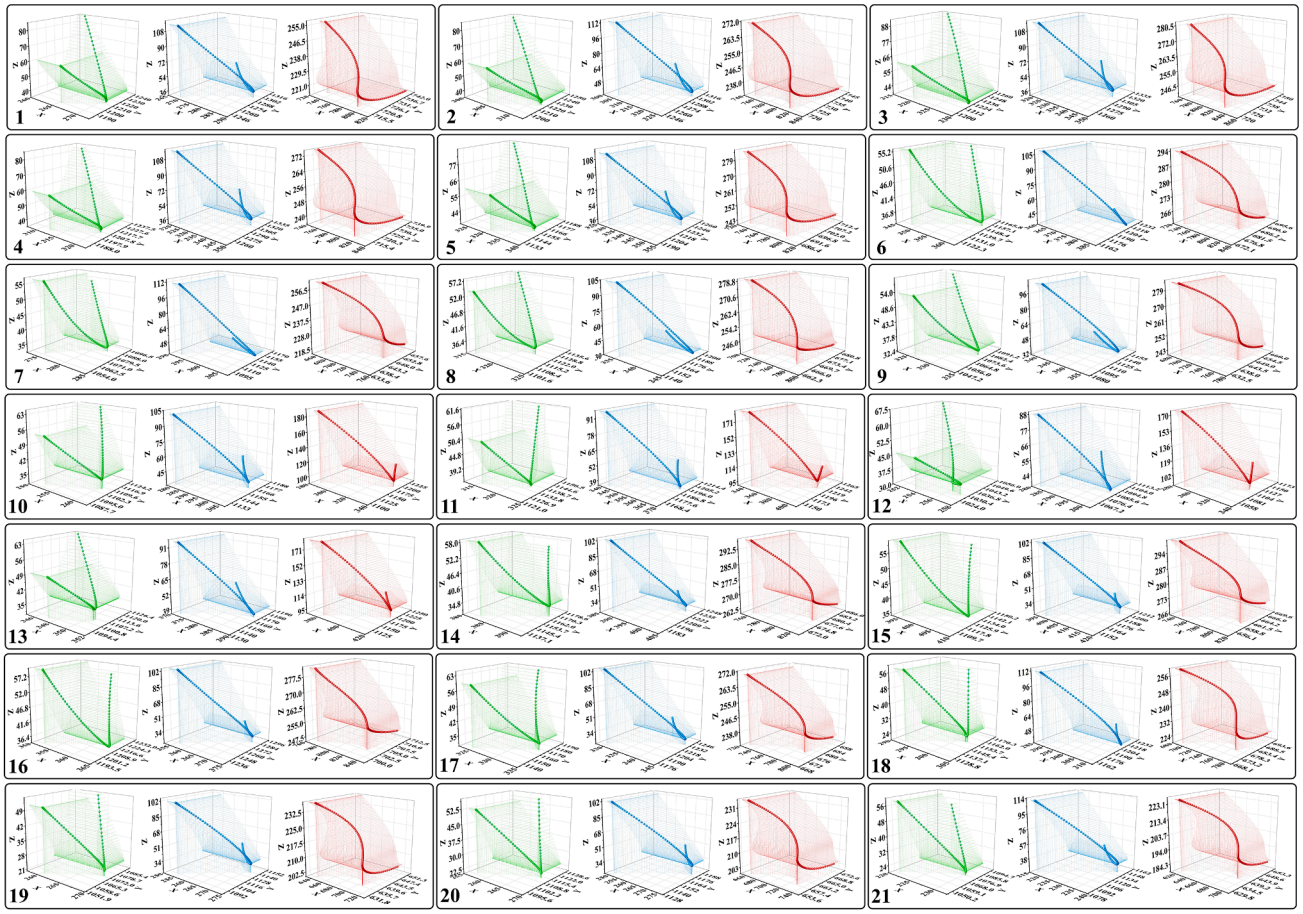

**Figure 3. The spatial displacements 21 after fracture subjects**

The spatial displacements of three parts of foot segments in a group of 21 after fracture subjects during the running stance phase. Green: forefoot; blue: midfoot; red: rearfoot.

Researchers have found that people with MT5 fractures have significantly higher plantar pressures than people who do not have them, especially in the area of the first metatarsophalangeal joint.[28] While the study examined changes in static plantar pressure, we cannot entirely depend on its findings to support our theory. However, we can deduce from the results that changes in plantar pressure can cause MT1 stresses to increase. Upon comparing our findings with the available information, this deduction seems to make sense. In addition, it is not just the MT1 that experiences higher levels of stress in individuals who have had a fracture; this also happens in the MT2. This further suggests that a fracture of the lateral metatarsal, even after rehabilitation, can potentially affect changes in the medial metatarsal. In terms of sports anatomy, the foot is actually an unstable structure.[29] Previous studies have demonstrated that the unstable structure of the foot is more inclined to be medial-lateral unstable, which also further supports the results of the present study.[26,30] It also seems entirely possible that because of the structural changes in the lateral foot, the stresses in the medial foot will thus become greater. After a fracture, the sagittal ankle joint angle decreases, and the corresponding joint moment and joint power also decrease. This situation at the same running speed is likely due to the metatarsal bone's compensatory mechanism.

The results of the present study indicate that the MT4 stress was higher after the fracture than it was before. This raises a question, as our previous reasoning suggested that the high stress in the MT1 and MT2 was due to the foot's medial-lateral instability. And since the MT1 and MT2 have already compensated, why is the MT4 also under increased stress? From a running biomechanics point of view,[31,32] this seems logical, as the MT5 is the one closest to the ground, and the impact it receives is not negligible. However, if the MT4 does not undergo a compensatory mechanism concurrently with structural damage to the MT5, the entire foot structure may struggle to maintain stability, potentially leading to a completely different gait pattern. It can also be seen from the results in the Figure 5 that there are great differences in the biomechanical parameters of the two groups. In terms of the timing of the peak stress in MT1 and MT4, this would seem to further support our conjecture. Because of the structural damage to the MT5, the MT1 and

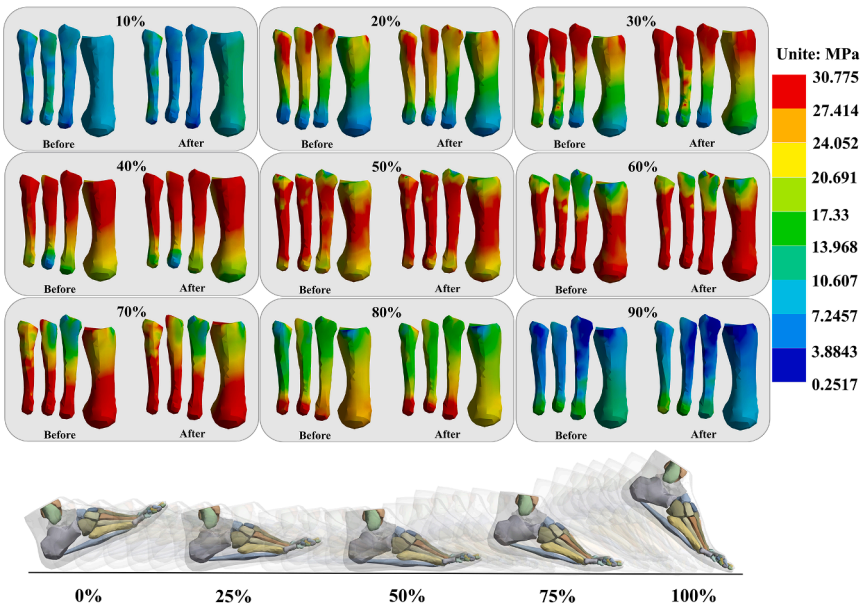


**Figure 4. The distribution of the Von-Mise stress**

The Von-Mises stress change of the MT1-4 from 10% to 90% running stance phase.

MT4 intervened early in the stance phase as a way to help compensate for the MT5 deficiencies.

From the stress changes in the MT1 before the fracture, it can be found that the peak stress in the MT1 occurs during the push-off phase stage. The results of the previous study[33] suggest that the big toe region should generate the most force under normal gait conditions. Instead, the peak MT stress changed considerably after the fracture, and we believe that the compensatory mechanism mentioned in the previous section is the important reason for this. The compensatory mechanism was applied to MT1, potentially leading to its early involvement in the entire stance phase. Another potential explanation could be that MT1 balances with MT4, which also requires compensation to ensure the stability of the entire foot. Finally, MT1 should have been the primary contributor to the push-off phase, but after the MT5 fracture, MT2 and MT3 took the lead for all the previously mentioned reasons. From the changes in muscle forces (Figure 5C), especially the muscles that control the ankle joint and metatarsophalangeal joint, we can further strengthen our conjecture.

In this study, the MT stress changes before fracture in the same situation were restored by using the internal displacement of the bone captured by DFIS as a boundary condition. This study found that when a fracture of the MT5 occurs, even after rehabilitation, there is a significant impact on the metatarsal. In addition, this study further found that when a fracture of the MT5 occurs, all of the MT bones make corresponding adjustments as a result of this structural change. Correspondingly, similar compensation mechanisms have been developed based on kinematics, kinetics, and muscle forces data to adapt to the changes caused by fractures. This study not only provides further insight into the foot after a fracture but also allows for the restoration of the before fracture condition as a means of judging the post-rehabilitation condition.

## Limitations of the study

Originally, the selection process for this study included a male participant. The conclusions derived from the study may differ because of inherent individual variability. Furthermore, variations in material property settings and boundary conditions can significantly influence the final results. In addition, to simplify the model, we set boundary conditions by dividing the foot into three parts and applying three collective displacements. However, a more effective approach would be to create the displacements bone-by-bone.

## RESOURCE AVAILABILITY

### Lead contact

Further information and request for resources and data should be directed to and will be fulfilled by the lead contact, Yaodong Gu (guyaodong@nbu.edu.cn).

### Materials availability

This study did not generate new unique materials.

### Data and code availability

- Data and code reported in this article will be shared by the lead contact upon request.
- All original code reported in this article will be shared by the lead contact upon request.
- Any additional information required to reanalyze the data reported in this article is available from the lead contact upon request.

## ACKNOWLEDGMENTS

This study was sponsored by Zhejiang Provincial Natural Science Foundation of China for Distinguished Young Scholars (LR22A020002), Zhejiang Provincial Key Research and Development Program of China (2023C03197), Ningbo key R&D Program (2022Z196), Zhejiang Province Exploring Public Welfare Projects (LTGY23H040003), Ningbo Natural Science Foundation (20221JCGY 010532 and 20221JCGY010607), Public Welfare Science & Technology Project of Ningbo, China (2021S134), and Zhejiang Rehabilitation Medical

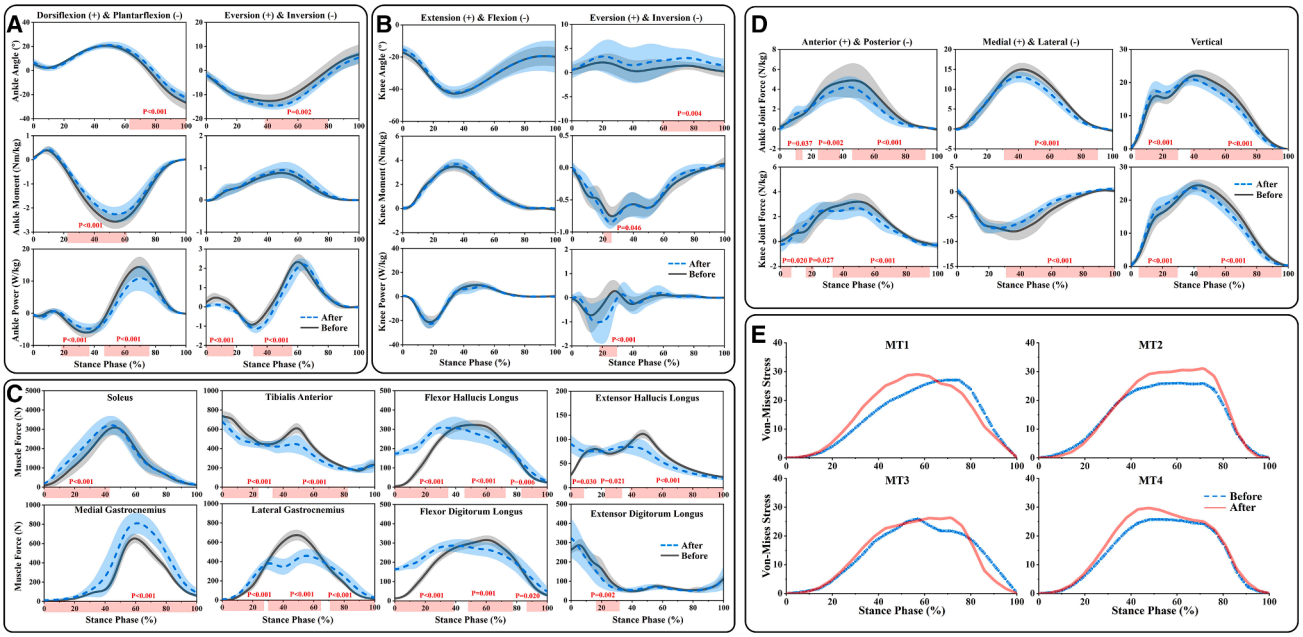


**Figure 5. Changes of biomechanical parameters**

(A) Changes in the ankle angle, ankle moment, and ankle power during the running stance phase for before and after fracture.

(B) Changes in the knee angle, knee moment and knee power during the running stance phase for before and after fracture.

(C) Changes in soleus, tibialis anterior, medial gastrocnemius, lateral gastrocnemius, flexor hallucis longus, extensor hallucis longus, flexor digitorum longus, and extensor digitorum longus during the running stance phase for before and after fracture.

(D) Changes in the ankle joint force and knee joint force during the running stance phase for before and after fracture.

(E) The Von-Mises stress change of the MT1-4 during the running stance phase for before and after fracture. The black solid line represents the average running stance phase of healthy subjects, and the gray shaded is the standard deviation; the blue dotted line represents the average running stance phase of subjects after fracture, and the blue shaded is the standard deviation; in each picture, the bottom shows the running stance phase from 0% to 100%; the red shading indicates that there is a significant difference in the data at this stage, and the red font is the specific significant difference value.

Association Scientific Research Special Fund (ZKKY2023001). We express our heartfelt gratitude for this.

## AUTHOR CONTRIBUTIONS

Conceptualization, H.Z., D.X., Z.G., and Y.G.; methodology, H.Z., D.X., W.Q., and L.X.; software, H.Z., W.Q., Z.G., and Y.G.; validation, H.Z., W.Q., D.X., and Z.G.; investigation, H.Z., Z.G., and Y.G.; writing—original draft preparation, H. Z., D.X., and W.Q.; writing—review and editing, L.X. and Y.G.; all authors have read and agreed to the published version of the manuscript.

## DECLARATION OF INTERESTS

The authors declare no competing interests.

## STAR★METHODS

Detailed methods are provided in the online version of this paper and include the following:

- KEY RESOURCES TABLE
- EXPERIMENTAL MODEL AND STUDY PARTICIPANT DETAILS
  - Participants
- METHOD DETAILS
  - Biomechanics parameters collection
- QUANTIFICATION AND STATISTICAL ANALYSIS
  - Model Reconstruction
  - Boundary and loading condition
  - Statistical analysis

## SUPPLEMENTAL INFORMATION

Supplemental information can be found online at https://doi.org/10.1016/j.isci.2025.112432.

Received: July 25, 2024
Revised: November 1, 2024
Accepted: April 10, 2025
Published: April 15, 2025

## REFERENCES

1. Van Middelkoop, M., Kolkman, J., Van Ochten, J., Bierma-Zeinstra, S., and Koes, B.W. (2008). Risk factors for lower extremity injuries among male marathon runners. Scand. J. Med. Sci. Sports *18*, 691–697.
2. Estok, P.J., and Rudy, E.B. (1987). Marathon running: comparison of physical and psychosocial risks for men and women. Res. Nurs. Health *10*, 79–85.
3. Koplan, J.P., Rothenberg, R.B., and Jones, E.L. (1995). The natural history of exercise: a 10-yr follow-up of a cohort of runners. Med. Sci. Sports Exerc. *27*, 1180–1184.
4. Powell, K.E., Kohl, H.W., Caspersen, C.J., and Blair, S.N. (1986). An epidemiological perspective on the causes of running injuries. Physician Sportsmed. *14*, 100–114.
5. Herrera-Soto, J.A., Scherb, M., Duffy, M.F., and Albright, J.C. (2007). Fractures of the fifth metatarsal in children and adolescents. J. Pediatr. Orthop. *27*, 427–431.

6. Owen, R.J., Hickey, F.G., and Finlay, D.B. (1995). A study of metatarsal fractures in children. Injury *26*, 537–538.
7. Petrisor, B.A., Ekrol, I., and Court-Brown, C. (2006). The epidemiology of metatarsal fractures. Foot Ankle Int. *27*, 172–174.
8. Singer, G., Cichocki, M., Schalamon, J., Eberl, R., and Höllwarth, M.E. (2008). A study of metatarsal fractures in children. JBJS *90*, 772–776.
9. Dameron, T.B., Jr. (1975). Fractures and anatomical variations of the proximal portion of the fifth metatarsal. JBJS *57*, 788–792.
10. Quill, G.E., Jr. (1995). Fractures of the proximal fifth metatarsal. Orthop. Clin. N. Am. *26*, 353–361.
11. Brilakis, E., Kaselouris, E., Xypnitos, F., Provatidis, C.G., and Efstathopoulos, N. (2012). Effects of foot posture on fifth metatarsal fracture healing: a finite element study. J. Foot Ankle Surg. *51*, 720–728.
12. Hicks, J. (1954). The mechanics of the foot: II. The plantar aponeurosis and the arch. J. Anat. *88*, 25–30.
13. Hicks, J. (1953). The mechanics of the foot: I. The joints. J. Anat. *87*, 345–357.
14. Chruscik, A., Kauter, K., Windus, L., Whiteside, E., and Dooley, L. (2021). Fundamentals of anatomy and physiology (University of Southern Queensland), pp. 765–767.
15. Bennett, M.R., Harris, J.W.K., Richmond, B.G., Braun, D.R., Mbua, E., Kiura, P., Olago, D., Kibunjia, M., Omuombo, C., Behrensmeyer, A.K., et al. (2009). Early hominin foot morphology based on 1.5-million-year-old footprints from Ileret, Kenya. Science *323*, 1197–1201.
16. Lieberman, D.E. (2012). Those feet in ancient times. Nature *483*, 550–551.
17. Engelke, K., van Rietbergen, B., and Zysset, P. (2016). FEA to measure bone strength: a review. Clin. Rev. Bone Miner. Metabol. *14*, 26–37.
18. Ratchev, S., Liu, S., Huang, W., and Becker, A.A. (2006). An advanced FEA based force induced error compensation strategy in milling. Int. J. Mach. Tool Manufact. *46*, 542–551.
19. Horstemeyer, M.F. (2012). Integrated Computational Materials Engineering (ICME) for Metals: Using Multiscale Modeling to Invigorate Engineering Design with Science (John Wiley & Sons), pp. 354–355.
20. Jain, M.L., Govind Dhande, S., and Vyas, N.S. (2011). Virtual modeling of an ankle foot orthosis for correction of foot abnormality. Robot. Comput. Integrated Manuf. *27*, 257–260.
21. Chantarapanich, N., Wongsiri, S., and Sitthiseripratip, K. (2019). Influence of insole slope on bone joint stress, foot bone stress, and foot pressure distribution. Songklanakarin J. Sci. Technol. *41*, 2.
22. Chantarapanich, N., Wongsiri, S., and Wanchat, S. (2021). Effect of insole-footwear combination on foot biomechanics: A finite element study. Engineering & Applied Science Research *48*, 6.
23. Murni, N.S., Dambatta, M.S., Yeap, S.K., Froemming, G.R.A., and Hermawan, H. (2015). Cytotoxicity evaluation of biodegradable Zn–3Mg alloy toward normal human osteoblast cells. Mater. Sci. Eng., C *49*, 560–566.
24. Ye, D., Sun, X., Zhang, C., Zhang, S., Zhang, X., Wang, S., and Fu, W. (2021). In vivo foot and ankle kinematics during activities measured by using a dual fluoroscopic imaging system: a narrative review. Front. Bioeng. Biotechnol. *9*, 693806.
25. Koo, T.K., and Li, M.Y. (2016). A guideline of selecting and reporting intraclass correlation coefficients for reliability research. J. Chiropr. Med. *15*, 155–163.
26. Zhou, H., Xu, D., Quan, W., Ugbolue, U.C., Zhou, Z., and Gu, Y. (2024). Can the Entire Function of the Foot Be Concentrated in the Forefoot Area during the Running Stance Phase? A Finite Element Study of Different Shoe Soles. J. Hum. Kinet. *92*, 5–17.
27. Picciano, A.M., Rowlands, M.S., and Worrell, T. (1993). Reliability of open and closed kinetic chain subtalar joint neutral positions and navicular drop test. J. Orthop. Sports Phys. Ther. *18*, 553–558.
28. Hetsroni, I., Nyska, M., Ben-Sira, D., Mann, G., Segal, O., Maoz, G., and Ayalon, M. (2010). Analysis of foot structure in athletes sustaining proximal fifth metatarsal stress fracture. Foot Ankle Int. *31*, 203–211.
29. Cavanagh, P.R., Morag, E., Boulton, A.J., Young, M.J., Deffner, K.T., and Pammer, S.E. (1997). The relationship of static foot structure to dynamic foot function. J. Biomech. *30*, 243–250.
30. Zhou, H., and Ugbolue, U.C. (2024). Biomechanical analysis of lower limbs based on unstable condition sports footwear: a systematic review. Physical Activity and Health *8*, 93–104.
31. Nicola, T.L., and Jewison, D.J. (2012). The anatomy and biomechanics of running. Clin. Sports Med. *31*, 187–201.
32. Novacheck, T.F. (1998). The biomechanics of running. Gait Posture *7*, 77–95.
33. Nagel, A., Fernholz, F., Kibele, C., and Rosenbaum, D. (2008). Long distance running increases plantar pressures beneath the metatarsal heads: a barefoot walking investigation of 200 marathon runners. Gait Posture *27*, 152–155.
34. Li, G., Van de Velde, S.K., and Bingham, J.T. (2008). Validation of a non-invasive fluoroscopic imaging technique for the measurement of dynamic knee joint motion. J. Biomech. *41*, 1616–1622.
35. Knörlein, B.J., Baier, D.B., Gatesy, S.M., Laurence-Chasen, J., and Brainerd, E.L. (2016). Validation of XMALab software for marker-based XROMM. J. Exp. Biol. *219*, 3701–3711.
36. De Asla, R.J., Kozánek, M., Wan, L., Rubash, H.E., and Li, G. (2009). Function of anterior talofibular and calcaneofibular ligaments during in-vivo motion of the ankle joint complex. J. Orthop. Surg. Res. *4*, 1–6.
37. Zhou, H., Xu, D., Quan, W., Ugbolue, U.C., Sculthorpe, N.F., Baker, J.S., and Gu, Y. (2022). A foot joint and muscle force assessment of the running stance phase whilst wearing normal shoes and bionic shoes. Acta Bioeng. Biomech. *24*, 191–202.
38. Delp, S.L., Anderson, F.C., Arnold, A.S., Loan, P., Habib, A., John, C.T., Guendelman, E., and Thelen, D.G. (2007). OpenSim: open-source software to create and analyze dynamic simulations of movement. IEEE Trans. Biomed. Eng. *54*, 1940–1950.
39. Faul, F., Erdfelder, E., Buchner, A., and Lang, A.G. (2009). Statistical power analyses using G*Power 3.1: Tests for correlation and regression analyses. Behav. Res. Methods *41*, 1149–1160.

# STAR★METHODS

## KEY RESOURCES TABLE

| REAGENT or RESOURCE | SOURCE | IDENTIFIER |
|---|---|---|
| Other | | |
| Kistler force plate | Kistler Ltd. | https://www.kistler.com/ |
| Vicon motion capture system | Oxford Metrics Ltd. | https://www.vicon.com/ |
| Dual fluoroscopic imaging system | Taoimage Medical Technology Ltd. | https://www.taoimage.com/ |

## EXPERIMENTAL MODEL AND STUDY PARTICIPANT DETAILS

### Participants

A total of 21 subjects (Table S1) had previously experienced a shaft stress fracture of the MT5 in the six months before the collection of experimental data. All patients received treatment through the use of cast immobilization for a duration of 4–6 weeks. After the subject's recovery, we obtained gait biomechanical data. At the same time, we also obtained gait data from 21 healthy subjects (Table S1) as the control group. A male Chinese participant with experienced a shaft stress fracture of the MT5 (age: 28 years) was enlisted for the FE analysis. This study focused on analyzing rearfoot striking patterns. All methods were performed in accordance with the Declaration of Helsinki. After obtaining a detailed description of the research's objective and methods, the participant gave written permission to affirm their well-informed choice to participate. The Ethics Committee of Ningbo University approved this study (protocol code: TY2024022).

## METHOD DETAILS

### Biomechanics parameters collection

The study employed a Kistler force platform and an eight-camera Vicon motion capture system (Oxford Metrics Ltd., Oxford, UK) to collect data on the dynamics and kinematics. Figure S1A illustrates the location of 39 markers. The participant advanced and sprinted along a 10-meter track at a velocity of 5 m/s in order to capture the rearfoot running stance phase of the right foot (Figure S1B). The current study employed OpenSim software, developed by Stanford University in Stanford, CA, USA, to calculate biomechanical parameters for subsequent FE analysis. Surface muscle activations and forces were recorded using EMG equipment (Delsys, Boston, MA, USA).

## QUANTIFICATION AND STATISTICAL ANALYSIS

### Model Reconstruction

A CT and MRI scan were performed on the right foot of the participant (tube voltage: 120 kV, tube current: 125 mA, slice thickness: 2 mm; no interval scanning). The two-dimensional image was divided into segments using Mimics 21.0 (Materialise, Leuven, Belgium). The bone, plantar fascia, and bulk soft tissue were refined using Geomagic Studio 2021 (Geomagic, Inc., Research Triangle Park, NC, United States). The software SolidWorks 2017, developed by SolidWorks Corporation in Waltham, MA, United States, was utilized to assemble the components and subsequently convert them into solid objects. A solid material has been developed to mimic the composition of cartilage, which fills the space between two neighboring bones. The before fracture structure (healthy foot) was fitted by displacing two parts of MT5 and combining them into a single solid.

Two fluoroscopes were positioned at right angles to each other, 90° apart, in order to capture foot fluoroscopy images simultaneously from two different perspectives (anterolateral and anteromedial). A cubic calibration frame was used to establish the spatial calibration of the shooting area. The XMAlab software (Version 2.1.0, Brown University, Prov, USA) then determined the relative positions of the X-ray tube and the flat panel detector in space.[34] Afterward, the environment calibration file produced by XMAlab was imported into the 3-D modeling software Rhinoceros (Version 7.4, Robert McNeel Ltd., WA, USA) in order to establish a virtual biorthogonal perspective system.[34,35]

Two virtual cameras were created to simulate the X-ray sources of the two fluoroscopes, taking into account the placement of perpendicular fluoroscopic images in order to accurately recreate the position of the fluoroscopic enhancers (Figure S2). Subsequently, the foot model was imported into the virtual environment, and the bone position was modified through rotation and translation in Rhinoceros software to align the projected contour of the foot model with the actual bone position shown in the X-ray fluoroscopic images.[36] The 3-D model created in Mimics using foot MRI/CT data was utilized as a previously used framework for correcting and aligning the model. Ultimately, the coordinate systems for the forefoot, midfoot, and rearfoot were established,

and the coordinate system calculator plug-in in Rhinoceros was used to calculate three relative displacements of different parts of the foot.[35]

### Boundary and loading condition

An LS-DYNA dynamic solver from Workbench 2021 (ANSYS, Inc. located in Canonsburg, PA, USA) was used to perform a simulation of the running stance phase (before and after fracture). The mesh size of each solid was controlled by the program (Figure S1D). The Workbench program enabled the automatic identification of component interactions. An algorithm based on surface closeness was used to determine potential contact pairings. The bone surface and cartilage were simulated to interact physically by making direct face-to-face contact. The bone's surface established a frictionless connection with the cartilage. The enclosed soft tissue functioned as an anchor for both the bones and cartilage. A contact surface with a friction coefficient of 0.6 was used to simulate the interaction between the foot and the ground (Figure S1C).

Figure S1C outlines the biomechanical parameter indicators that are subjected to loading. First, fix the ground, and set and define the position of the foot model. In the FE model, the ankle joint angle was set by adjusting the angle between the tibial axis and the longitudinal axis of the foot on the sagittal plane. The global coordinate system remained consistent with the original coordinate system of OpenSim.[37,38] Finally, the displacements derived from the three parts of foot assemblies are added to the model as a further setting of the boundary conditions. All materials, except for the encapsulated soft tissue and skin were assumed to be isotropic and linear elastic materials, and their properties were obtained from prior research. Table S2 enumerates the material properties of each part.

### Statistical analysis

The dataset was subjected to Shapiro-Wilk normality tests prior to statistical analysis. Paired t-tests were utilized to compare running stance phases between two pairs of shoes, and no significant differences were discovered. All data from the walking and running phases were retrieved, and the data of the stance phase was stretched into a time series curve of 101 data points using a custom script of MATLAB for SPM). Open source SPM1d paired-samples t-tests software was utilized for the statistical analysis. The significance threshold $p$-value was set at 0.05. A statistical power analysis was performed, with the use of G*Power,[39] which indicated a sample size needed of 20 patients at least for each group to detect moderate differences.